Article

Cell

Spontaneous Activity of Cochlear Hair Cells Triggered by Fluid Secretion Mechanism in Adjacent Support Cells

Graphical Abstract

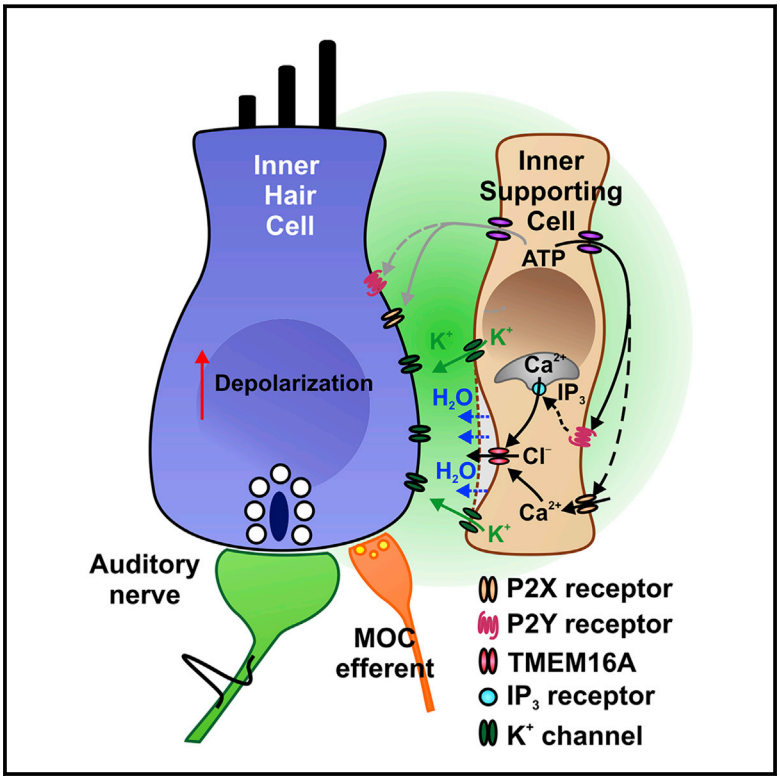

Authors

Han Chin Wang, Chun-Chieh Lin, Rocky Cheung, ..., Graham Ellis-Davies, Jason Rock, Dwight E. Bergles

Correspondence

dbergles@jhmi.edu

In Brief

Glia-like support cells in the developing cochlea use a fluid secretion pathway that causes cell shrinkage to trigger periodic excitation of inner hair cells.

Highlights

- Inner supporting cells (ISCs) in the developing cochlea express TMEM16A Cl^- channels
- Spontaneous currents in ISCs reflect purinergic receptor-mediated gating of TMEM16A
- Cl^- efflux through TMEM16A induces K^+ release, which depolarizes inner hair cells
- Spontaneous activity of hair cells and ganglion neurons is reduced in Tmem16a KO mice

Wang et al., 2015, Cell *163*, 1348–1359
December 3, 2015 ©2015 Elsevier Inc.
http://dx.doi.org/10.1016/j.cell.2015.10.070

Cell

Article

Spontaneous Activity of Cochlear Hair Cells Triggered by Fluid Secretion Mechanism in Adjacent Support Cells

Han Chin Wang,[1] Chun-Chieh Lin,[1] Rocky Cheung,[1,5] YingXin Zhang-Hooks,[1] Amit Agarwal,[1] Graham Ellis-Davies,[2] Jason Rock,[3] and Dwight E. Bergles[1,4,*]

[1]Solomon H. Snyder Department of Neuroscience, Johns Hopkins University School of Medicine, 725 North Wolfe Street, WBSB 1001, Baltimore, MD 21205, USA

[2]Department of Neuroscience, Mount Sinai School of Medicine, One Gustave Levy Place Box 1065, New York, NY 10029, USA

[3]Department of Anatomy, University of California, San Francisco, 513 Parnassus Ave, Box 0452, San Francisco, CA 94143, USA

[4]Department of Otolaryngology-Head and Neck Surgery, Johns Hopkins School of Medicine, 725 N. Wolfe Street, Baltimore, MD 21205, USA

[5]Present address: Department of Chemistry and Biochemistry, University of California, Los Angeles, 611 Charles E Young Dr East, Boyer Hall Room 456, Los Angeles, CA 90095, USA

*Correspondence: dbergles@jhmi.edu

http://dx.doi.org/10.1016/j.cell.2015.10.070

SUMMARY

Spontaneous electrical activity of neurons in developing sensory systems promotes their maturation and proper connectivity. In the auditory system, spontaneous activity of cochlear inner hair cells (IHCs) is initiated by the release of ATP from glia-like inner supporting cells (ISCs), facilitating maturation of central pathways before hearing onset. Here, we find that ATP stimulates purinergic autoreceptors in ISCs, triggering Cl^- efflux and osmotic cell shrinkage by opening TMEM16A Ca^{2+}-activated Cl^- channels. Release of Cl^- from ISCs also forces K^+ efflux, causing transient depolarization of IHCs near ATP release sites. Genetic deletion of TMEM16A markedly reduces the spontaneous activity of IHCs and spiral ganglion neurons in the developing cochlea and prevents ATP-dependent shrinkage of supporting cells. These results indicate that supporting cells in the developing cochlea have adapted a pathway used for fluid secretion in other organs to induce periodic excitation of hair cells.

INTRODUCTION

Neurons in developing sensory systems exhibit robust spontaneous electrical activity, which promotes their survival and maturation as well as the targeting and refinement of their projections (Blankenship and Feller, 2010; Kirkby et al., 2013; Moody and Bosma, 2005). This intrinsic activity is initiated within sensory organs, ensuring that functional pathways are established between the periphery and the brain centers responsible for processing modality-specific information. By establishing these nascent networks prior to the appearance of sensory input, the nervous system provides an appropriate substrate for experience-dependent plasticity. However, the molecular mechanisms responsible for inducing neural activity within these structures remain poorly understood. Uncovering these mechanisms may help reveal the causes of developmental sensory impairment that arise from genetic or environmental factors and provide new ways of ameliorating behavioral problems precipitated by deficits in sensory processing.

In the developing auditory system, neurons exhibit periodic bursts of action potentials prior to hearing onset, a phenomenon that is conserved from birds to mammals (Wang and Bergles, 2015). Prior studies have shown that ablation of the cochlea or peripheral block of action potentials in the auditory nerve abolishes burst firing in central auditory centers (Lippe, 1994; Tritsch et al., 2010a), indicating that spontaneous activity originates within the developing cochlea. Although inner hair cells (IHCs) can fire spontaneous Ca^{2+} spikes at this age (Kros et al., 1998; Sendin et al., 2014; Tritsch and Bergles, 2010), non-neuronal, supporting cells appear to play a crucial role in generating the periodic, high-frequency bursts of activity observed in auditory centers of the brain (Tritsch et al., 2007).

The inner supporting cells (ISCs) responsible for initiating spontaneous activity in the prehearing cochlea form a pseudo-stratified epithelium known as Kölliker's organ (greater epithelial ridge) that lies immediately adjacent to IHCs. ATP is released spontaneously from ISCs, which ultimately results in excitation of IHCs, glutamate release, and bursts of action potentials in spiral ganglion neurons (SGNs) that propagate to central auditory centers (Tritsch et al., 2010a; Tritsch et al., 2007). This spontaneous release of ATP also activates purinergic autoreceptors in ISCs, triggering a rise in intracellular Ca^{2+}, a large inward current, and transient shrinkage (crenation) of groups of ISCs near sites of ATP release. It has been assumed that the responses of supporting cells and hair cells to ATP represent parallel, functionally distinct consequences of purinergic receptor activation. However, the mechanism by which ATP induces excitation of IHCs has not been determined.

Here, we demonstrate that supporting cells in the prehearing cochlea induce periodic excitation of IHCs by activating transmembrane protein 16A (TMEM16A; also know as Anoctamin-1, ANO1) Ca^{2+}-activated Cl^- channels (CaCCs). Our studies indicate that Ca^{2+} transients resulting from activation of purinergic autoreceptors trigger opening of TMEM16A channels in ISCs. The efflux

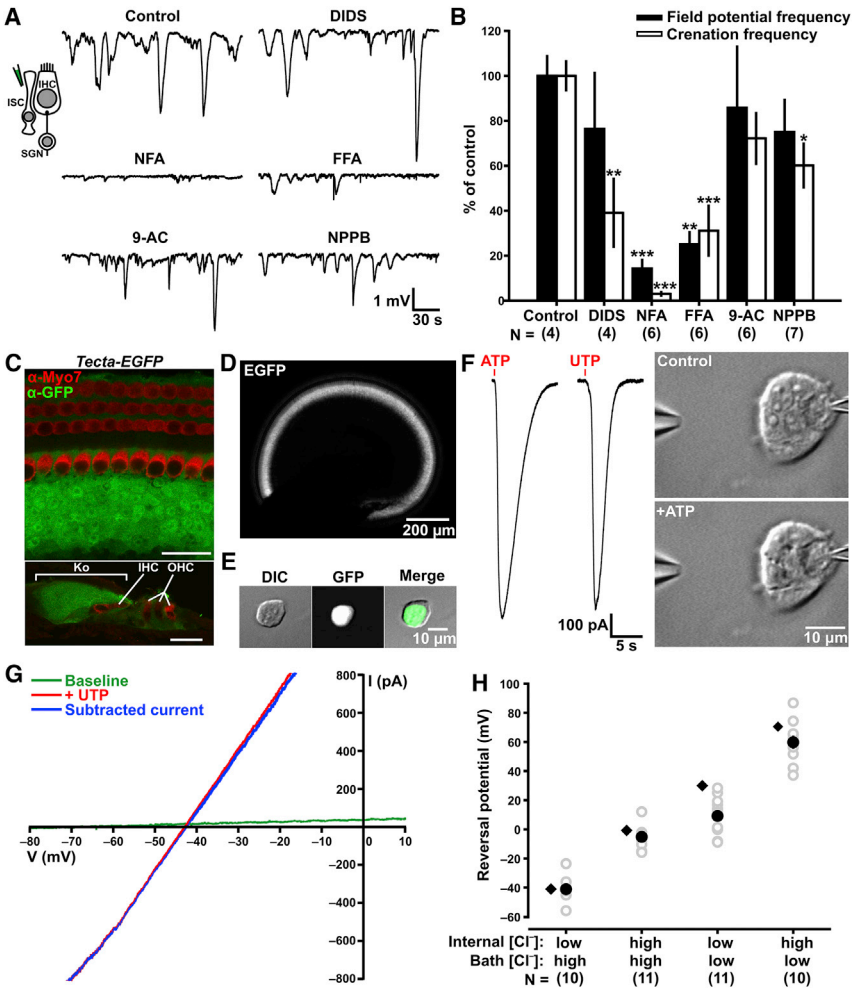

Figure 1. Spontaneous Currents in ISCs Are Mediated by Chloride Channels

(A) Extracellular field potential recordings from Kölliker's organ (P8 rats). DIDS: 4,4'-Diisothiocyano-2,2′-stilbenedisulfonic acid (250 μM); NFA: niflumic acid (300 μM); FFA: flufenamic acid (100 μM); 9-AC: 9-anthracenecarboxylic acid (1 mM); NPPB: 5-Nitro-2-(3-phenylpropylamino) benzoic acid (50 μM). Inset: recording configuration.

(B) Histogram showing changes in field potential fluctuations and crenations in the presence of Cl^- channel blockers. Data shown as mean ± SEM. n = number of cochlear turns. *p < 0.05; **p < 0.01; ***p < 0.001, one way ANOVA.

(C) Expression of GFP in a whole mount (upper) and cross section (lower) of the organ of Corti from P7 *Tecta-EGFP* mice. Scale bar: 20 μm. Ko: Kölliker's organ. OHC: outer hair cell.

(D) Whole mount of the organ of Corti from a P8 *Tecta-EGFP* mouse showing endogenous GFP.

(E) Differential interference contrast (DIC) imaging and endogenous GFP signals in a cell cluster after dissociation (P7 *Tecta-EGFP* mouse).

(F) Exogenous nucleotide-evoked currents (left) and crenation (right) from small clusters of dissociated ISCs.

(G) Current-voltage (I-V) relationship of membrane currents from dissociated ISCs measured at baseline (green) and during exogenous UTP stimulation (red). UTP-induced current (difference between two conditions) is shown in blue.

(H) Reversal potential of UTP-induced currents in ISCs measured in response to changes in the Cl^- equilibrium potential (E_{Cl}, ◆). Data shown as mean ± SEM. n = number of clusters.

See also Movie S1.

of Cl^- through TMEM16A channels is followed by efflux of both water (causing crenation) and K^+. The resulting elevation of extracellular K^+ depolarizes IHCs and induces repetitive firing. TMEM16A is highly enriched in ISCs that contact IHCs, and expression of this channel matches the developmental changes in spontaneous activity exhibited by IHCs. Moreover, genetic deletion of TMEM16A abolished ATP-induced currents in ISCs, prevented ISC crenation, and markedly reduced spontaneous burst firing in both IHCs and SGNs. These studies indicate that a mechanism used by epithelial cells to enable ion secretion in other organs (Frizzell and Hanrahan, 2012) is used by supporting cells in the developing cochlea to trigger neuronal activity in the auditory system before hearing onset.

RESULTS

Spontaneous Currents in ISCs Are Mediated by the Opening of Chloride Channels

Spontaneous release of ATP from ISCs triggers a rise in intracellular Ca^{2+}, membrane depolarization, and crenation through activation of purinergic autoreceptors. This rise in $[Ca^{2+}]_i$ is sufficient to induce both depolarization and crenation (Tritsch et al., 2010b), suggesting that gating of a Ca^{2+}-dependent conductance is a key step in ISC activation. ATP activates a Cl^- current in outer supporting cells (Hensen's cells) in the cochlea (Sugasawa et al., 1996), and crenation of ISCs is inhibited by a Cl^- channel inhibitor (Tritsch et al., 2010b); as transmembrane flux of Cl^- is typically accompanied by osmotically driven water movement (Frizzell and Hanrahan, 2012), gating of a Ca^{2+}-dependent Cl^- conductance could account for both effects of purinergic receptor activation. To explore this possibility, we examined the sensitivity of these responses to several broad spectrum Cl^- channel inhibitors. Both spontaneous field potential fluctuations recorded within Kölliker's organ, which arise from currents in ISCs (Tritsch et al., 2007), and crenation of ISCs, were markedly reduced by Cl^- channel antagonists (Figures 1A and 1B). However, these antagonists also inhibit purinergic receptors and gap junctions (Burnstock and Williams, 2000; Eskandari et al., 2002), necessitating direct measurements of the conductance change induced by purinergic receptor activation.

ISCs are extensively coupled to other supporting cells by gap junctions (Jagger and Forge, 2006), reducing the ability to control membrane voltage and precluding manipulations of intracellular ion concentrations. To overcome these limitations, we examined

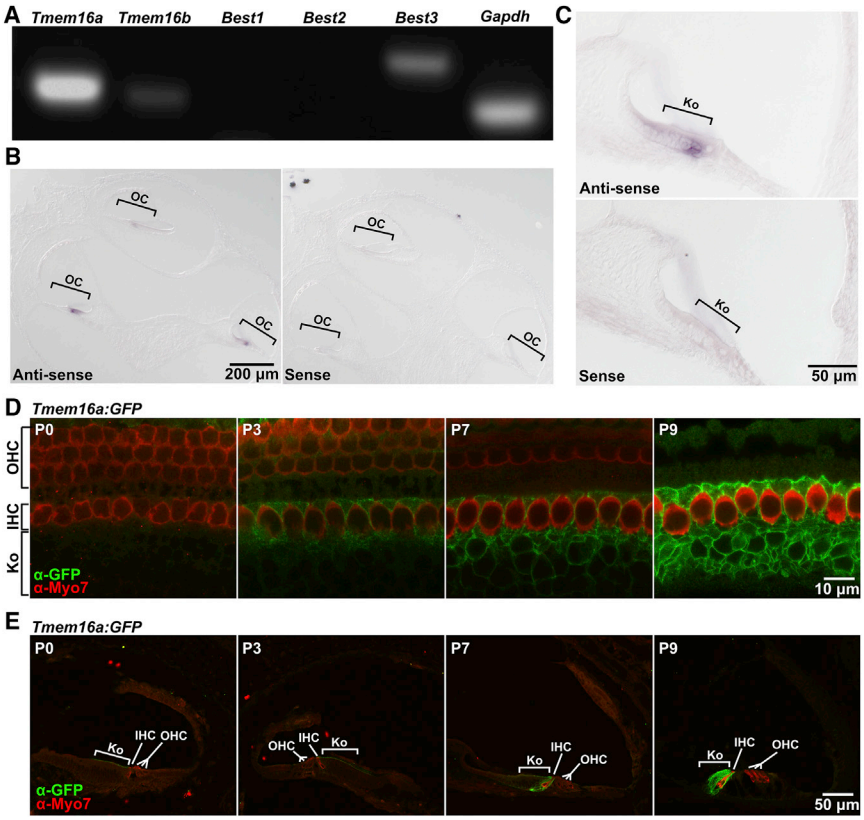

Figure 2. The Ca^{2+}-Activated Cl^- Channel TMEM16A Is Highly Expressed by ISCs

(A) RT-PCR detection of CaCC mRNAs in the sensory epithelium of P7 mouse cochleae. *Gapdh* was used as positive control.

(B) In situ hybridization of *Tmem16a* mRNA in the cochlea of a P7 mouse. Sense probe (right) was used as negative control. OC: organ of Corti.

(C) In situ hybridization of *Tmem16a* mRNA in the organ of Corti from a P7 mouse. Ko: Kölliker's organ.

(D) Expression of TMEM16A through early development in whole mounts of the organ of Corti.

(E) Expression of TMEM16A through early development in cross sections of the organ of Corti.

See also Figure S1.

purinergic receptor-induced responses in acutely isolated ISCs. To identify ISCs after dissociation, we developed a bacterial artificial chromosome (BAC) transgenic mouse line in which expression of EGFP is controlled by the promoter for α-tectorin, which is secreted by ISCs to help form the tectorial membrane (Rau et al., 1999). EGFP is highly expressed by ISCs in *Tecta-EGFP* mice, with much lower levels present in Deiters' cells (Figures 1C and 1D). ISCs survived as small clusters of three to six cells following isolation (Figure 1E), which remained gap junction coupled, allowing control of the membrane potential, intracellular ion substitution, and assessments of crenation. Focal application of ATP or the P2Y receptor-specific agonist uridine triphosphate (UTP) to EGFP-expressing ISC clusters elicited large inward currents (>1 nA) and crenation (Figure 1F and Movie S1), recapitulating the behavior of ISCs in the intact cochlea. Although ISCs exhibited a low membrane conductance at rest (membrane resistance: 2.07 ± 0.68 GΩ, n = 42 ISC clusters), their membrane conductance was dramatically enhanced by exposure to UTP, as assessed by performing continuous sweeps of membrane voltage before and during UTP stimulation (Figure 1G). The UTP-induced current reversed at −41.1 ± 2.5 mV (n = 10), close to the predicted Cl^- equilibrium potential (E_{Cl} = −41.3 mV) and shifting E_{Cl} to more positive potentials by varying intracellular and extracellular Cl^- induced positive shifts in the reversal potential that matched the predicted E_{Cl} (Figure 1H). As epithelial cells maintain a high intracellular concentration of Cl^- (Frizzell and Hanrahan, 2012) and ISCs have a highly negative resting membrane potential (∼−90 mV), opening of these Cl^- channels results in Cl^- efflux and depolarization, followed by crenation, as expected if Cl^- efflux is accompanied by water efflux (Hoffmann et al., 2009). Together, these results suggest that CaCCs are primarily responsible for these forms of ISC activity in the prehearing cochlea.

The Ca^{2+}-Activated Cl^- Channel TMEM16A Is Highly Expressed by ISCs

Two families of CaCCs have been identified, the bestrophins and Tmem16; among these, only BEST1-3, TMEM16A, and TMEM16B have been shown to function as CaCCs (Huang et al., 2012a). RT-PCR analysis of the sensory epithelium of cochleae isolated at postnatal day 7 (P7, day of birth as P0), a time when ISCs exhibit robust spontaneous activity, revealed high expression of *Tmem16a* mRNA and low expression of *Best3* mRNA (Figure 2A), a finding corroborated by the enrichment of *Tmem16a* mRNA in non-hair cells, as assessed by RNA-seq (Scheffer et al., 2015). In situ hybridization indicated that *Tmem16a* mRNA is restricted to ISCs in the developing sensory epithelium (Figures 2B and 2C). We further examined TMEM16A expression in the cochlea using a mouse line in which GFP-tagged TMEM16A was knocked in to the *Tmem16a* gene locus (*Tmem16a:GFP*; Huang et al., 2012b). Analysis of these *Tmem16a:GFP* mice revealed that expression of TMEM16A is confined to Kölliker's organ in the cochlea (Figures S1A and S1B), a finding supported by immunocytochemical labeling (Yi et al., 2013), and was most highly expressed by ISCs that surround IHCs (Figures 2D and 2E). No GFP expression was detected in IHCs (Figures S1C and S1D). This medial to lateral increase in TMEM16A expression coincides with the spatial distribution of spontaneous crenations in Kölliker's organ (Tritsch et al., 2010b). The expression of TMEM16A increased markedly during the first 2 postnatal weeks and then declined after hearing onset (Figures 2D, 2E, and S1E), consistent with the developmental progression of spontaneous activity in ISCs (Tritsch et al., 2010b). Thus, TMEM16A is well positioned to contribute to the activity observed in ISCs in the prehearing cochlea.

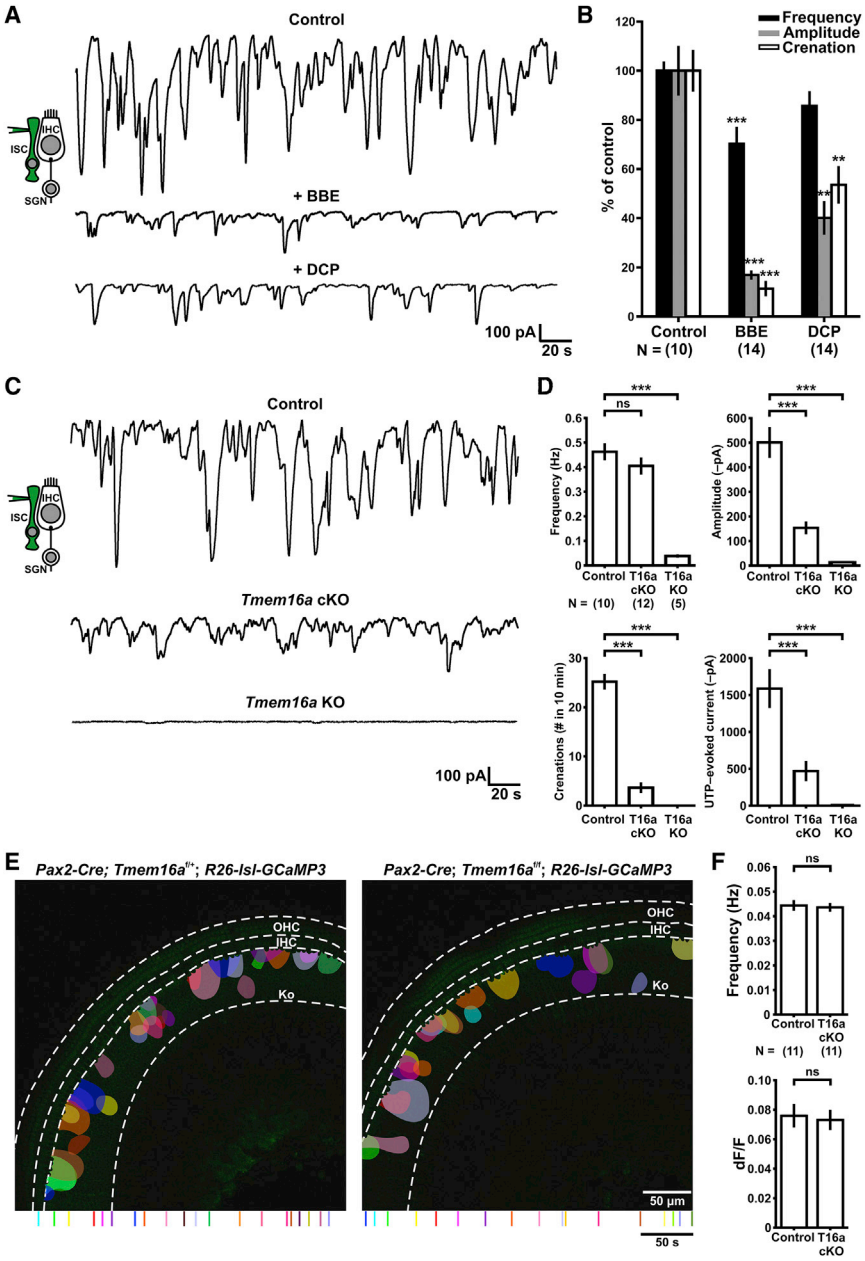

Figure 3. TMEM16A Is Required for Spontaneous Currents and Cremations in ISCs

(A) Whole-cell voltage clamp recordings from P9 rat ISCs in control and in TMEM16A inhibitors. BBE: 10 μM; DCP: 20 μM. Inset: recording configuration.

(B) Quantification of spontaneous currents and cremations in ISCs in the presence of TMEM16A inhibitors. Data shown as mean ± SEM. n = number of cochlear turns. **p < 0.01; ***p < 0.001, one way ANOVA.

(C) Whole-cell voltage clamp recording from P7 mouse ISCs from control, *Tmem16a* cKO, and *Tmem16a* KO mice.

(D) Quantification of spontaneous currents, spontaneous cremations, and UTP-evoked currents in ISCs from control, *Tmem16a* cKO, and *Tmem16a* KO mice. Data shown as mean ± SEM. n = number of animals. ***p < 0.001; ns: not significant, one way ANOVA.

(E) Maps showing maximum area of spontaneous Ca^{2+} transients in ISCs of control (left) and *Tmem16a* cKO (right) mice (300 s imaging period). Raster plot indicating the timing of individual Ca^{2+} transients in ISCs is shown at the bottom.

(F) Quantification of spontaneous Ca^{2+} transients in the ISCs in control and *Tmem16a* cKO mice. Data shown as mean ± SEM. n = number of animals. ns: not significant, one way ANOVA.

See also Figure S2 and Movies S2 and S3.

TMEM16A Is Required for Spontaneous Currents in ISCs

To determine if TMEM16A is responsible for the Ca^{2+}-activated Cl^- current in ISCs, we recorded spontaneous activity in ISCs in the presence of TMEM16A inhibitors benzbromarone (BBE) and dichlorophen (DCP) (Huang et al., 2012b). Consistent with the enriched expression of TMEM16A in ISCs, both inhibitors significantly suppressed spontaneous currents and cremations (Figures 3A and 3B). We also generated *Tmem16a* conditional null mutant mice (*Tmem16a* cKO) by crossing *Tmem16a*$^{f/f}$ mice (Schreiber et al., 2015) with *Pax2-Cre* mice (Ohyama and Groves, 2004). These *Pax2-Cre* mice induce widespread recombination in the developing cochlea. Conditional removal of TMEM16A markedly reduced spontaneous currents, UTP-evoked currents, and ISC cremation (Figures 3C and 3D). Although some residual activity was observed, this may reflect incomplete removal of TMEM16A, as the efficiency of the *Pax2-Cre* mouse line is approximately 80% (Freyer et al., 2011). Indeed, areas of focal TMEM16A immunoreactivity remained in Kölliker's organ in *Tmem16a* cKO mice and infrequent cremations occurred (Figure S2 and Movie S2). Although complete knockout (KO) of *Tmem16a* results in neonatal lethality due to impaired respiratory system (Rock et al., 2008), we were able to analyze ISC activity from *Tmem16a*-null mutant mice (*Tmem16a* KO) that survived until P7. Spontaneous and UTP-evoked currents and cremations were nearly absent in ISCs from *Tmem16a* KO cochleae (Figures 3C and 3D), suggesting that this channel is primarily responsible for both P2 receptor-mediated events. To assess whether loss of these channels affects spontaneous release of ATP or expression of purinergic receptors, which would similarly abolish activity, we monitored spontaneous Ca^{2+} transients in Kölliker's organ by expressing the genetically encoded Ca^{2+} sensor GCaMP3 in the *Tmem16a* cKO background (*Pax2-Cre;Tmem16a*$^{f/f}$*;R26-lsl-GCaMP3* mice) (Paukert et al., 2014). Confocal time-lapse imaging revealed that there was no difference in spontaneous Ca^{2+} transients between control (*Pax2-Cre;Tmem16a*$^{f/+}$*;R26-lsl-GCaMP3*) and *Tmem16a* cKO mice (Figures 3E

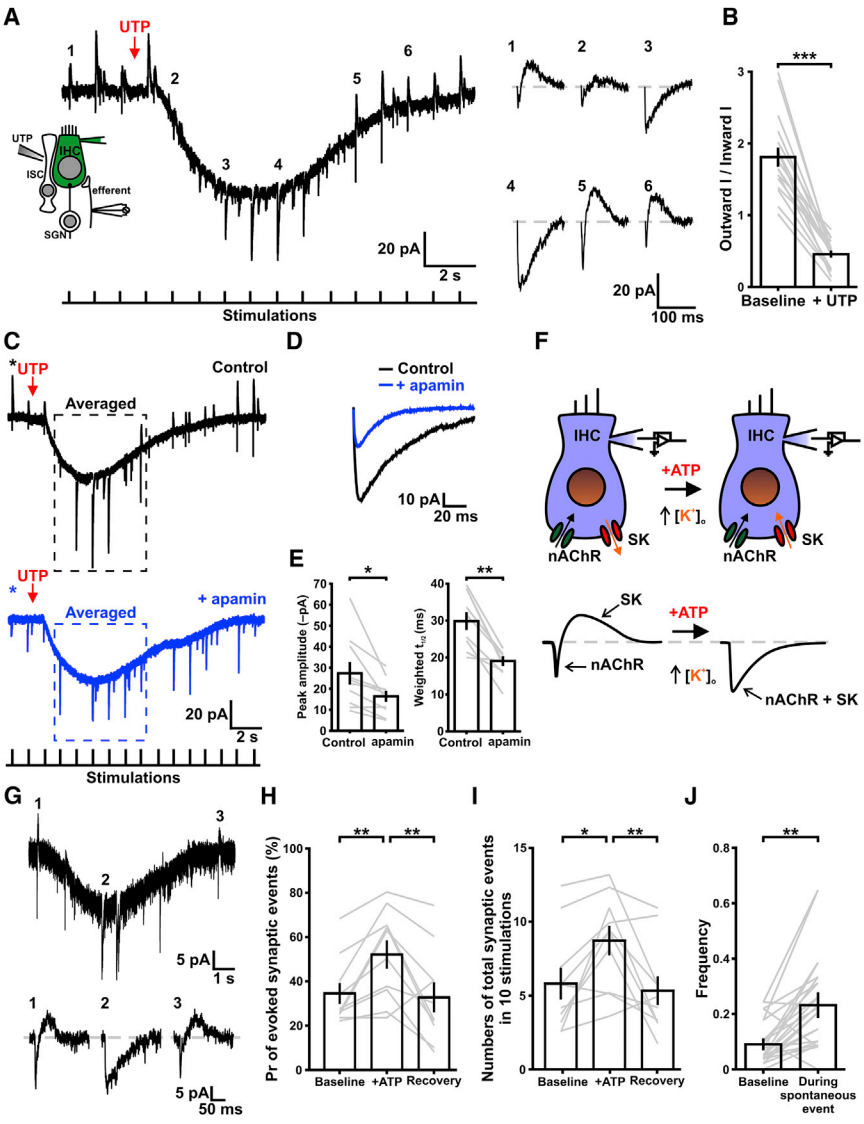

Figure 4. Extracellular K^+ Levels Increase around IHCs during Spontaneous Activity

(A) Whole-cell recording from an IHC showing the slow inward current induced by UTP and the accompanying transient change in waveform of efferent synaptic currents.

(B) Quantification of the ratio of outward current to inward current of efferent synaptic currents. Data shown as mean ± SEM. ***$p < 0.001$, n = 17 cells, paired two-tail Student's t test.

(C) Whole-cell recording from an IHC showing the response to UTP in the presence of the SK channel inhibitor apamin (300 nM, blue trace). *: Baseline outward current was blocked by apamin.

(D) Comparison of the averaged waveform of evoked efferents near the peak of UTP-induced currents from cell in (C).

(E) Quantification of evoked efferents that occurred near the peak of UTP-induced currents in control and in apamin. Data shown as mean ± SEM. *$p < 0.05$; **$p < 0.01$. n = 10 cells, paired two-tail Student's t test.

(F) Model illustrating the change in efferent waveform during purinergic stimulation caused by a shift in the direction of K^+ flow through SK channels.

(G) Whole-cell recording from an IHC showing the change in spontaneous efferent waveform during a spontaneous inward current. V_m was held at −92 mV (closer to E_K) to highlight the alteration in E_K.

(H) Probability (Pr) of successfully evoking efferent synaptic currents during ATP-evoked events. Experiments were performed at near physiological temperature (~34°C–36°C). Data shown as mean ± SEM. **$p < 0.01$, n = 10 cells, one way repeated-measures ANOVA with Bonferroni test.

(I) Plot of the number of evoked and spontaneous efferent synaptic currents elicited by 10 consecutive stimulations (1 Hz), highlighting increase in release probability during ATP. Data shown as mean ± SEM. *$p < 0.05$; **$p < 0.01$, n = 10 cells, one way repeated-measures ANOVA with Bonferroni test.

(J) Histogram showing frequency of spontaneous efferent synaptic currents during spontaneous ATP release events. Experiments were performed at ~34°C–36°C. Data shown as mean ± SEM. **$p < 0.01$, n = 13 cells, paired two-tail Student's t test.

See also Figure S3.

and 3F and Movie S3), indicating that removal of TMEM16A does not disrupt the spontaneous release of ATP, expression of P2Y receptors, or the ability of these receptors to mobilize intracellular Ca^{2+}. Together, these results indicate that TMEM16A is responsible for the ATP-mediated increase in Cl^- conductance in ISCs and that Cl^- efflux through these channels is required for crenation.

Extracellular K^+ Levels Increase around IHCs during Spontaneous Activity

TMEM16A has been shown to participate in Cl^- secretion from various exocrine epithelia (Huang et al., 2012a). In these tissues, Cl^- efflux is accompanied by the efflux of both water and K^+ to maintain osmotic and ionic gradients, respectively (Frizzell and Hanrahan, 2012). These findings raise the possibility that purinergic receptor activation in ISCs may also induce K^+ efflux, leading to an increase in the concentration of K^+ outside IHCs. To test this hypothesis, we utilized small conductance Ca^{2+}-activated K^+ (SK) channels in IHCs to sense the local K^+ concentration surrounding IHCs. SK channels are activated when acetylcholine is released from medial olivocochlear (MOC) efferent synapses. Cholinergic synaptic currents are normally biphasic, reflecting Na^+/Ca^{2+} influx through $\alpha9/\alpha10$ nicotinic receptors and K^+ efflux through SK channels, which are activated by the Ca^{2+} that enters through these receptors (Glowatzki and Fuchs, 2000). If $[K^+]_o$ increases, the outward K^+ current through SK channels should decrease. Focal application of UTP to Kölliker's organ triggered a prolonged inward current in nearby IHCs voltage clamped at their resting potential (~−82 mV) (Figure 4A), similar to spontaneous events (Tritsch et al., 2007). The waveform of efferent

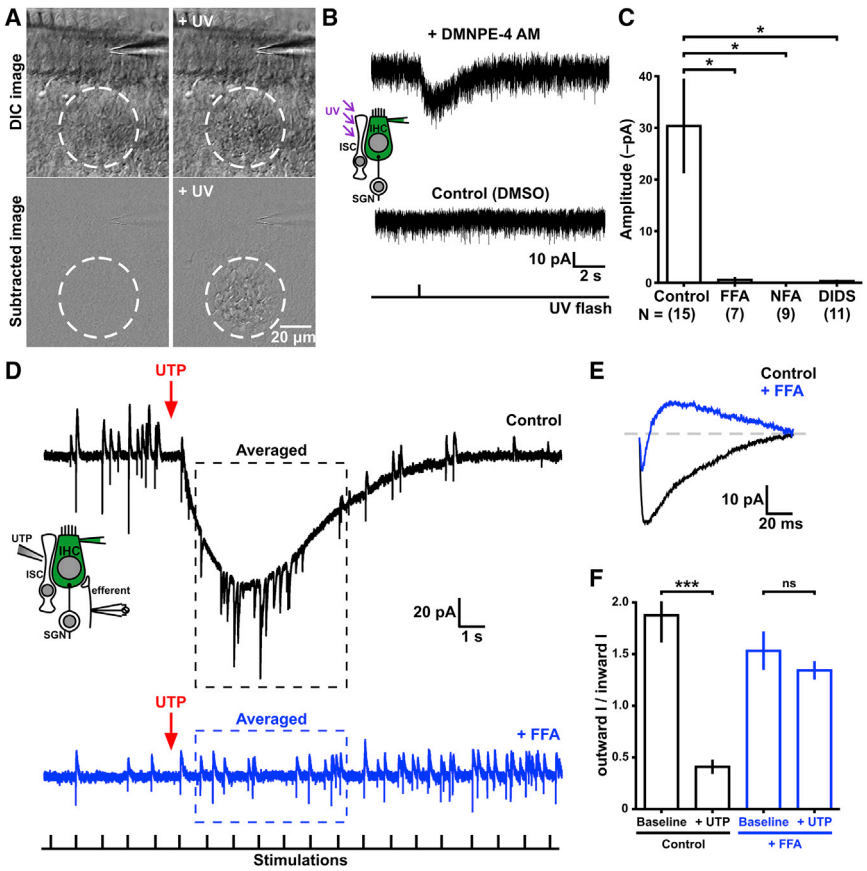

Figure 5. K^+ Release from ISCs Is Sufficient to Excite IHCs

(A) DIC images showing response of ISCs before (left panel) and after UV illumination when cochleae were loaded with caged Ca^{2+} (DMNPE-4/AM, 20 µM). White dashed circle indicates region of laser illumination.

(B) Whole-cell recordings from IHCs showing responses to UV illumination of Kölliker's organ in cochleae loaded with caged Ca^{2+} (DMNPE-4/AM, top) or vehicle (DMSO, bottom). Superfusing solution contained PPADS. Inset: recording configuration.

(C) Quantification of Ca^{2+} uncaging-induced currents in IHCs. FFA: 100 µM; NFA: 300 µM; DIDS: 250 µM. Data shown as mean ± SEM. n = number of cochlear turns. *p < 0.05, one way ANOVA.

(D) Whole-cell voltage clamp recording from an IHC illustrating response to UTP recorded in the absence (black trace) or presence of the Cl^- channel inhibitor FFA (100 µM, blue trace). Inset: recording configuration. Efferent synaptic currents were elicited through repetitive electrical stimulation at 1Hz.

(E) Averaged waveform of evoked efferent synaptic currents recorded at time of peak of UTP-induced current from cell in (D).

(F) Quantification of the ratio of outward current to inward current of evoked efferents at baseline and during UTP-induced current in control (black column) and FFA (blue column). Data shown as mean ± SEM. ***p < 0.001; ns: not significant, n = 8 cells, paired two-tail Student's t test.

See also Figure S4.

synaptic currents changed dramatically during the UTP-induced current, from biphasic during baseline to entirely inward at the peak of the response, and eventually returned to biphasic as the current returned to baseline (Figures 4A and 4B); a similar phenomenon was observed when ATP was applied (Figure S3). Synaptic currents at the peak of the UTP-evoked response were smaller and decayed faster in the SK channel inhibitor apamin (Figures 4C–4E), demonstrating that SK channel-mediated currents flowed inward during purinergic stimulation (Figure 4F). Moreover, at the peak of spontaneous slow inward currents in IHCs, synaptic currents also became monophasic inward (Figure 4G), indicating that there is a depolarizing shift in E_K when endogenous ATP is released from nearby ISCs. The probability of evoked acetylcholine release from efferent terminals was also significantly increased when ATP was applied (Figure 4H), and the frequency of spontaneous efferent synaptic currents was increased by exogenous (Figure 4I) and endogenous ATP (Figure 4J); as expected if these terminals are depolarized by the elevation in extracellular K^+.

K^+ Release from ISCs Is Sufficient to Excite IHCs

IHCs in the prehearing cochlea also express P2 receptors (Huang et al., 2010; Ito and Dulon, 2010) (Figure S4), and spontaneous depolarizations of IHCs are sensitive to P2 receptor antagonists (Tritsch et al., 2007). To assess whether K^+ release from ISCs is sufficient to depolarize IHCs without purinergic receptor activation, we activated TMEM16A directly by inducing a rise in intracellular Ca^{2+} within ISCs. ISCs were loaded with caged Ca^{2+} (DMNPE-4/AM) (Gordon et al., 2008) and whole-cell currents were recorded from IHCs in the presence of the P2 receptor antagonist PPADS to prevent direct excitation by ATP. IHCs lacked spontaneous inward currents before photorelease of Ca^{2+}, verifying that P2 receptor activation was blocked. When ISCs were focally illuminated with UV light, ISCs crenated (Figure 5A), as expected if TMEM16A was activated. When whole-cell recordings were made from an IHC and Ca^{2+} was liberated within nearby ISCs, a slow inward current was induced that was abolished by Cl^- channel antagonists (Figures 5B and 5C), indicating that K^+ release from ISCs is sufficient to activate IHCs and that K^+ release is dependent on Cl^- movement. When Cl^- channels were blocked, application of UTP no longer elicited an inward current in IHCs (Figure 5D), and the waveform of efferent synaptic currents remained biphasic during UTP stimulation (Figures 5E and 5F).

If elevation of extracellular K^+ is primarily responsible for depolarizing IHCs, then inhibiting K^+ channels in IHCs should attenuate their spontaneous activity. When whole-cell recordings were made from IHCs with an intracellular solution containing Cs^+ and tetraethylammonium (TEA), which blocks many, but not all K^+ channels, the amplitudes of spontaneous inward currents were reduced by 66% (Figures 6A and 6B), and the response to UTP was reduced by 82% (Figure 6C). This manipulation did

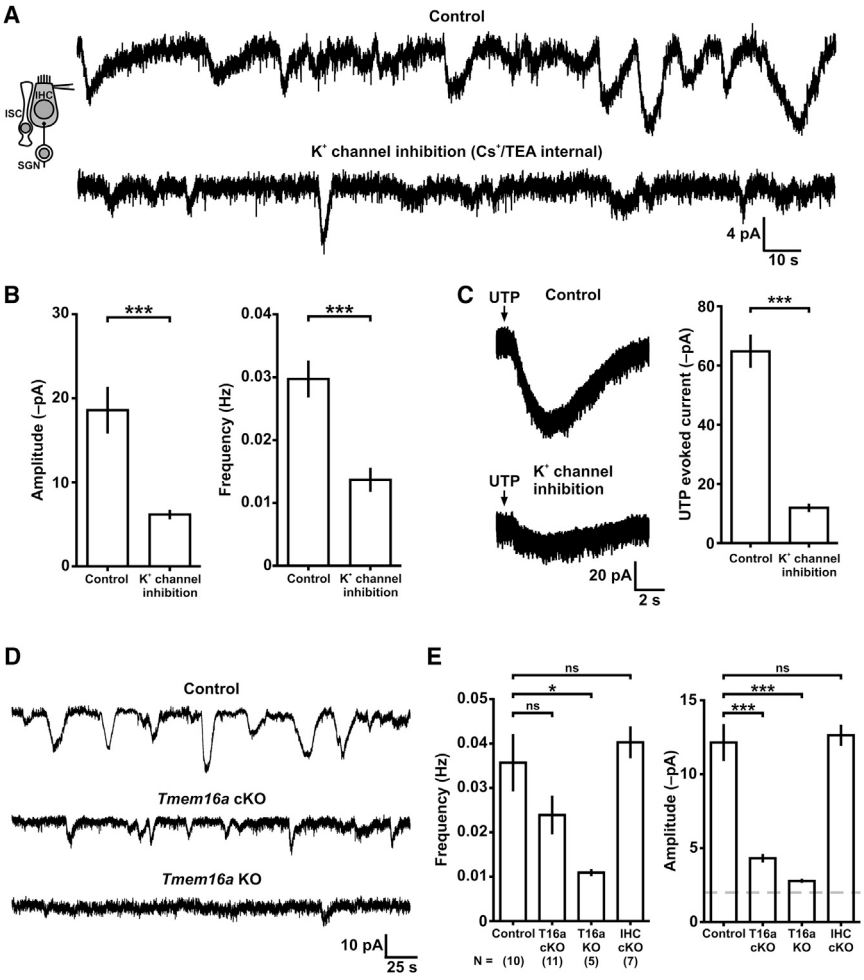

Figure 6. TMEM16A Is Required for K^+-Induced Excitation of IHCs

(A) Whole-cell voltage clamp recording of spontaneous currents from neighboring rat IHCs using a K^+-based intracellular solution (upper trace) or an intracellular solution containing Cs^+ and TEA (lower trace). Inset: recording configuration

(B) Quantification of spontaneous currents in neighboring rat IHCs recorded in control and with intracellular K^+ channel inhibition. Data shown as mean ± SEM. ***$p < 0.001$, $n = 23$ neighbor pairs of IHCs, paired two-tail Student's t test.

(C) Left: Whole-cell voltage clamp recordings from neighboring rat IHCs showing UTP-evoked currents obtained using a K^+-based intracellular solution (upper trace) or intracellular solution containing Cs^+ and TEA (lower trace). Right: Quantification of the amplitude of UTP-evoked currents. Data shown as mean ± SEM. ***$p < 0.001$, $n = 14$ neighbor pairs of IHCs, paired two-tail Student's t test.

(D) Whole-cell voltage clamp recordings of spontaneous inward currents in IHCs of control, *Tmem16a* cKO and *Tmem16a* KO mice.

(E) Quantification of spontaneous currents in IHCs of control, *Tmem16a* cKO, *Tmem16a* KO, and hair cell-specific *Tmem16a* cKO mice (IHC cKO). Gray dashed line indicates the level of noise in the recording. Data shown as mean ± SEM. n = number of animals. *$p < 0.05$; ***$p < 0.001$; ns: not significant, one way ANOVA.

not alter the frequency of ISC crenations (crenations/10 min, control: 14.1 ± 1.6; IHC K^+ channel inhibition: 13.2 ± 0.9, $p = 0.59$, paired t test), indicating that endogenous ATP release and ISC activity were unaffected. Because P2 receptors are not inhibited by intracellular Cs^+ or TEA (Burnstock, 2007), these results suggest that the elevation of $[K^+]_o$ during spontaneous activity is the primary force responsible for IHC depolarization.

If Cl^- efflux through TMEM16A is required to alter extracellular K^+ and induce slow inward currents in IHCs, then deletion of this channel should abolish this activity. In accordance with this hypothesis, spontaneous inward currents in IHCs were markedly reduced in cochleae from both *Tmem16a* cKO and *Tmem16a* KO mice (Figures 6D and 6E). Furthermore, the waveform of efferent synaptic currents no longer changed in *Tmem16a* KO mice when UTP was applied (Figure S3), indicating that the depolarizing shift in E_K depends on TMEM16A. IHCs did not appear to express GFP in *Tmem16a:GFP* mice (Figures S1C and S1D), and IHCs in cochleae from mice in which TMEM16A was selectively deleted from hair cells (*Atoh1-Cre;Tmem16a*$^{f/f}$) exhibited spontaneous activity that was indistinguishable from control (Figure 6E). The small currents that persisted in IHCs in *Tmem16a* KO mice may arise from direct activation of P2X receptors in IHCs (Figure S4). Together, these results indicate that release of K^+ from ISCs following TMEM16A activation is primarily responsible for inducing spontaneous inward currents in IHCs.

To estimate the magnitude of the $[K^+]_o$ increase experienced by IHCs following purinergic receptor activation, we compared IHC depolarizations induced by UTP and endogenous ATP to depolarizations induced by stepwise shifts in extracellular K^+ (Figures S5A and S5B). These results suggest that after UTP stimulation $[K^+]_o$ increased to 13.03 ± 0.45 mM (Figures S5A and S5B) and that 46% of spontaneous depolarizations are produced by $[K^+]_o$ increases that exceed 6 mM (Figure S5C). K^+ release from ISCs appears to be mediated through leak K^+ channels, as no outward current was elicited in response to UTP when TMEM16A channels were inhibited by BBE (n = 16 dissociated ISC clusters, data not shown), as would be expected if purinergic receptor activation triggers opening of K^+ channels.

TMEM16A-Induced K^+ Flux Increases IHC Burst Firing

To determine if TMEM16A is required to elicit IHC burst firing, we made current clamp recordings from IHCs in cochleae isolated from control (*Tmem16a*$^{f/f}$), *Tmem16a* cKO, and *Tmem16a* KO mice, using the perforated patch technique. Consistent with the reduction in spontaneous currents, the frequency of spontaneous Ca^{2+} spikes in IHCs was markedly reduced in *Tmem16a*

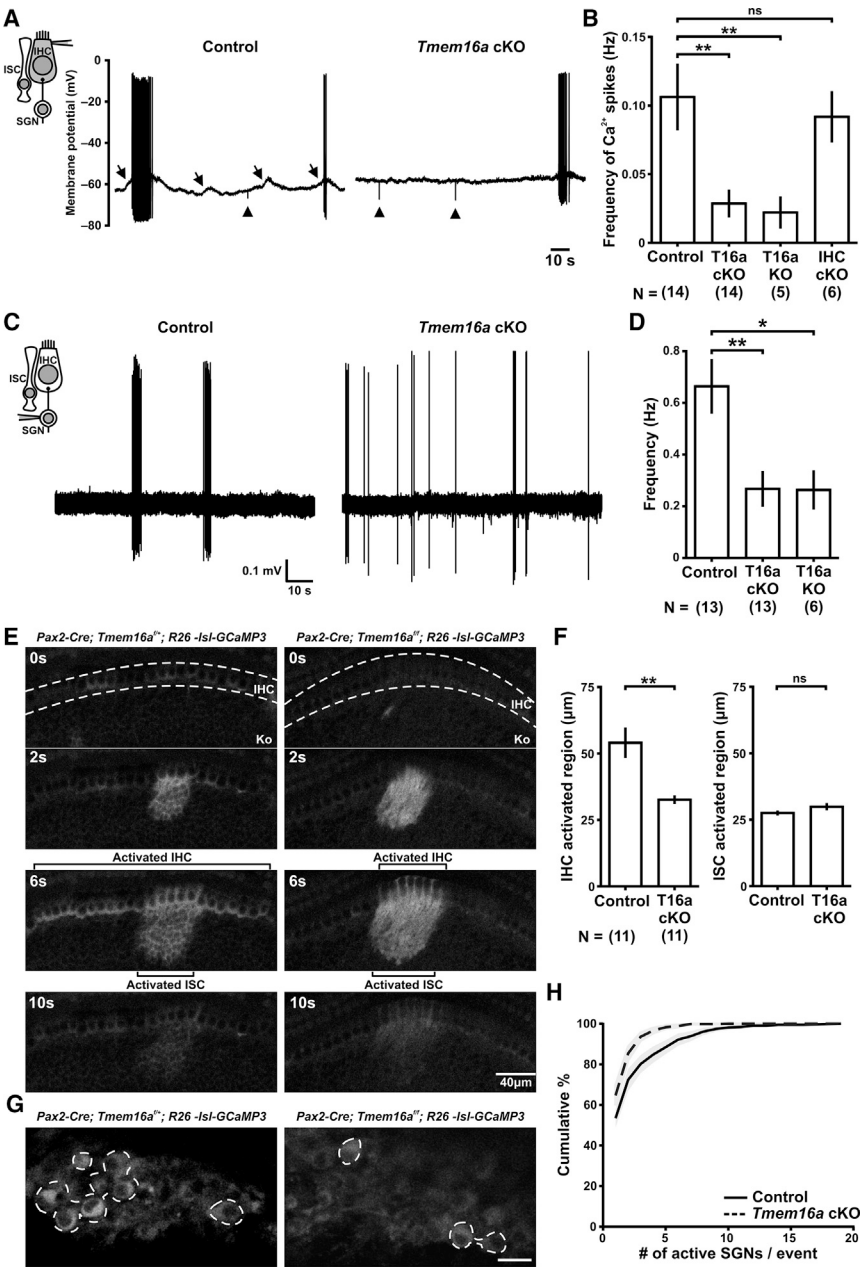

Figure 7. Removal of TMEM16A Reduces the Frequency and Synchronization of IHCs and SGNs

(A) Spontaneous Ca^{2+} spikes recorded from IHCs in control and *Tmem16a* cKO mice. Arrow: spontaneous depolarizations; arrowhead: spontaneous efferent synaptic currents. Inset: recording configuration.

(B) Quantification of spontaneous Ca^{2+} spikes from IHCs in control *Tmem16a* cKO, *Tmem16a* KO, and IHC cKO. Data shown as mean ± SEM. n = number of animals. **p < 0.01, ns: not significant, one way ANOVA.

(C) Spontaneous action potentials recorded from SGNs in control and *Tmem16a* cKO mice using cell-attached recording. Inset: recording configuration.

(D) Quantification of spontaneous action potentials from SGNs in control, *Tmem16a* cKO, and *Tmem16a* KO mice. Data shown as mean ± SEM. n = number of animals. *p < 0.05; **p < 0.01, one way ANOVA.

(E) Spontaneous Ca^{2+} transients from ISCs and IHCs in control (left) and *Tmem16a* cKO (right) mice monitored with GCaMP3. White dashed lines at 0 s highlight the border of the IHC region.

(F) Quantification of the region of activated IHCs and ISCs during spontaneous Ca^{2+} events. Only events that activated more than three IHCs were included in this analysis. Data shown as mean ± SEM. n = number of animals. **p < 0.01, ns: not significant, one way ANOVA.

(G) Spontaneous Ca^{2+} transients in SGNs of control (left) and *Tmem16a* cKO (right) mice monitored with GCaMP3. White dashed lines highlight activated SGNs. Scale bar: 10 μm.

(H) Plot of the cumulative percentage of activated SGNs during each spontaneous event. Data were pooled from 11 mice for control (solid line) and *Tmem16a* cKO (dashed line) mice. Gray borders indicate SEM p < 0.001, Kolmogorov-Smirnov Test.

See also Figures S5 and S6.

cKO and *Tmem16a* KO mice, but unaffected in hair cell-specific *Tmem16a* KO mice (Figures 7A and 7B), indicating that ISC TMEM16A channels promote IHC burst firing. Although there is uncertainty about the ambient concentration of K^+ that IHCs are exposed to before hearing onset, and recordings from IHCs are often performed in solutions containing 6 mM $[K^+]_o$, IHC excitation was still induced by K^+ release from ISCs when $[K^+]_o$ was increased to 6 mM in the superfusing solution (Figure S6A).

IHCs in the prehearing cochlea exhibit highly stereotyped bursts of Ca^{2+} spikes, in which the intervals between spikes within a burst progressively shorten and then lengthen during each burst, a consequence of the waveform of the underlying depolarizing stimulus (Tritsch et al., 2010a). Although bursts of Ca^{2+} spikes were observed in *Tmem16a* cKO mice, there were fewer long bursts (bursts containing >10 interspike intervals [ISIs]), ISIs within each burst were longer, and the magnitude of ISI interval change during each burst was reduced compared to control (Figures S6B and S6C), as expected if the amplitude and duration of each depolarization was reduced by removing TMEM16A. However, although the threshold for firing Ca^{2+} spikes was similar between control, *Tmem16a* cKO, and *Tmem16a* KO mice, the resting membrane potentials of IHCs in *Tmem16a* cKO and *Tmem16a* KO were more depolarized (Figures S6D and S6E). Therefore, any direct effect of ATP on IHCs would be more effective in these mice, suggesting that the contribution of TMEM16A to IHC excitation is underestimated in these mice.

TMEM16A-Dependent K^+ Efflux from ISCs Enhances Excitation of SGNs

Ca^{2+} spikes in IHCs elicit potent excitation of SGNs in the developing cochlea, as each Ca^{2+} spike elicits a mini-burst of up to six action potentials in postsynaptic SGNs (Tritsch et al., 2010a). To determine if removal of TMEM16A alters the firing behavior of SGNs, we made juxtacellular recordings from SGN somata in cochleae from *Tmem16a* mutants. SGNs from both *Tmem16a* cKO and *Tmem16a* KO mice exhibited fewer spontaneous action potentials than controls (Figures 7C and 7D), consistent with the reduction of Ca^{2+} spikes in IHCs. Moreover, SGNs in *Tmem16a* cKO mice exhibited fewer long bursts (bursts containing >10 ISIs) (Figure S6F), and ISIs within each burst were also longer (Figure S6G), in accordance with the change in the pattern of Ca^{2+} spikes in IHCs. Moreover, the second peak of ISI histogram, which represents the interval between mini-bursts, was shifted toward longer values in *Tmem16a* cKO mice (Figures S6H–S6J), mirroring the increase in the interval between successive Ca^{2+} spikes in IHCs. Thus, loss of TMEM16A reduces the overall activity of SGNs and disrupts their temporal firing pattern.

TMEM16A-Dependent K^+ Efflux from ISCs Promotes Synchronous Firing of IHCs and SGNs

To evaluate the role of TMEM16A in controlling synchronous activation of IHCs and SGNs, we monitored global activity patterns of IHCs and SGNs in *Pax2-Cre;R26-lsl-GCaMP3* mice, in which supporting cells, IHCs, and SGNs express GCaMP3. Spontaneous elevation of Ca^{2+} within groups of ISCs was associated with Ca^{2+} rises in a band of nearby IHCs (Figure 7E). The band of activated IHCs often extended well beyond the region of ISC activity, suggesting that K^+ may diffuse further than ATP. In *Tmem16a* cKO mice, fewer IHCs were activated during each ATP release event (control: 9.45 ± 1.03 IHCs/event; *Tmem16a* cKO: 5.64 ± 0.19 IHCs/event; n = 11, p = 0.002, one way ANOVA), and IHC activity was typically restricted to the region delimited by ISC activity (Figures 7E and 7F). The spread of Ca^{2+} transients among ISCs was unaffected in *Tmem16a* cKO mice, as expected if these events are determined by purinergic receptor activation rather than changes in $[K^+]_o$. Moreover, in *Tmem16a* cKO mice the number of SGNs that participated in each spontaneous event was significantly reduced (Figures 7G and 7H). Thus, disruption of ATP-induced K^+ release from ISCs not only decreases the overall activity of IHCs and SGNs, but also reduces the number of these cells that participate in each spontaneous event, altering the pattern of activity that is generated in the developing auditory system before hearing onset.

DISCUSSION

Excitable cells in the nervous system are ensheathed by glia, which provide metabolic support, restrict communication to intended partners, and maintain homeostasis by removing neurotransmitters and ions released during neuronal activity. Glial cells in the CNS such as astrocytes can also directly influence neuronal activity by releasing neuromodulatory factors (gliotransmitters), including ATP. However, much less is known about the neuromodulatory capabilities of glial cells in the periphery. Here, we show that supporting cells in the developing cochlea excite hair cells by inducing transient increases in extracellular K^+, exploiting a pathway that is used by epithelial cells throughout the body to secrete ions and water. A key step in this process involves activation of TMEM16A, a CaCC that sustains the large anion fluxes required to draw K^+ out of supporting cells. The concerted gating of these channels following activation of purinergic autoreceptors allows ISCs to induce correlated activity in auditory neurons that will ultimately respond to similar frequencies of sound, providing a means to promote activity-dependent refinement of auditory circuits before hearing onset.

TMEM16A Controls Ion and Water Release from Epithelial Cells in Diverse Tissues

The mammalian organ of Corti develops from epithelial progenitors in the ventromedial region of the otocyst (Kelley, 2006). Although hair cells and non-sensory supporting cells are specified and adopt their mosaic arrangement before birth, a large expanse of epithelial cells persists postnatally in a transient structure known as Kölliker's organ that lies immediately medial to IHCs. The columnar cells in Kölliker's organ exhibit characteristics of polarized epithelial cells in other tissues and establish intercellular tight junctions (Gulley and Reese, 1976) to limit paracellular diffusion and gap junctions to facilitate movement of ions and metabolites in the absence of blood vessels (Jagger and Forge, 2006). Although the dynamic behavior of ISCs described here may seem unusual, epithelial cells in the airway, intestine, and exocrine glands also initiate transmembrane ion flux to promote water and ion release. In these tissues, Cl^- is secreted into the lumen through apical Cl^- channels to establish an electrical driving force that promotes basolateral efflux of K^+ and paracellular movement of Na^+. The resulting extracellular accumulation of ions creates an osmotic gradient that forces water into the lumen (Frizzell and Hanrahan, 2012), triggering transient shrinkage (crenation) (Hoffmann et al., 2009). ATP and UTP are effective Cl^- secretagogues in respiratory epithelia, airway submucosal glands, conjunctival epithelia, pancreatic ducts, bile ducts, and intestinal epithelia (Novak, 2011), and purinergic receptor-mediated Cl^- secretion from these tissues often requires elevation of intracellular Ca^{2+} and activation of CaCCs (Novak, 2011). Moreover, recent studies indicate that TMEM16A participates in transepithelial Cl^- secretion from exocrine glands, mucus secretion from airway epithelia, and Ca^{2+}-dependent fluid secretion from bile ducts (Huang et al., 2012a). Thus, our studies indicate that epithelial cells in the developing cochlea use a common secretory pathway to initiate periodic excitation of IHCs.

Control of Extracellular K^+ by Glial Cells

Glial cells play a crucial role in maintaining extracellular K^+ levels within a narrow range, removing excess K^+ through channels and transporters and redistributing it to regions of lower concentration, a process facilitated by extensive gap junctional coupling within the glial syncytium (Kofuji and Newman, 2004). ISCs in the cochlea exhibit some features of astrocytes, including a highly negative resting potential, extensive gap junctional coupling (Jagger and Forge, 2006), as well as expression of purinergic receptors (Housley et al., 2009) and glutamate transporters (Glowatzki et al., 2006); however, several key differences allow K^+ to

accumulate outside ISCs. Although K^+ channels dominate the resting conductance of ISCs, the total K^+ conductance supported by these channels is low, limiting their ability to rapidly reabsorb K^+; most of their resting membrane conductance is mediated by gap junctions (Jagger and Forge, 2006), as treatment with gap junction blockers in situ or isolation of these cells increases their membrane resistance dramatically (see Figure 1G). ISCs also form tight junctions along their apical surface to restrict diffusion of K^+ between the cochlear epithelium and the endolymphatic compartment (Gulley and Reese, 1976).

Time-lapse imaging of intracellular Ca^{2+} changes in the cochlea revealed that IHC excitation spreads outward from the site of ATP release (defined by the location where Ca^{2+} first rises within ISCs), consistent with propagation of a wave of K^+ through the cochlear epithelium. IHCs were often activated over a much broader area than ISCs, an effect that was abolished by removal of TMEM16A (see Figures 7E and 7F), suggesting that the additional recruitment of IHCs arises from K^+-induced depolarization. K^+ may have the opportunity to influence a broader area than ATP, as the spread of ATP is constrained by extracellular nucleotidases (Housley et al., 2009). IHCs adjacent to ISCs were activated during ATP release events in *Tmem16a* cKO mice, presumably reflecting a direct effect of ATP on IHCs (see Figure S4). These findings indicate that concerted opening of TMEM16A channels in groups of ISCs markedly potentiates the action of ATP by increasing the number of synchronously active IHCs.

The Role of Supporting Cells in Generating Spontaneous Activity in the Developing Auditory System

Neurons in the auditory system of developing vertebrates exhibit brief periods of high-frequency firing followed by long periods of quiescence in the absence of sound. Synapses are formed between IHCs and SGNs several weeks before hearing onset (Sobkowicz et al., 1982), and SGN firing depends on synaptic input from IHCs during this period (Glowatzki and Fuchs, 2002; Tritsch and Bergles, 2010), suggesting that spontaneous burst firing depends on excitation of IHCs. This hypothesis is further supported by the highly stereotyped patterns of activity exhibited by central auditory neurons before hearing onset, which matches that induced in SGNs by IHCs (Tritsch et al., 2010a). Although the requirement for IHCs in burst firing is clear, the mechanisms responsible for inducing this activity have remained uncertain. One hypothesis is that IHCs are intrinsically active and that periodic interruption of their firing by efferent input or other neuromodulators is responsible for producing bursts (Kros, 2007), although recent studies indicate that burst firing of neurons in the medial nucleus of the trapezoid body (MNTB) persists in mice lacking α9 nicotinic receptor subunit (Clause et al., 2014), which abolishes efferent activity in IHCs. An alternative hypothesis is that IHCs are normally silent and that an external, excitatory stimulus initiates firing. Our previous studies suggest that the periodic release of ATP from ISCs could provide this stimulus (Tritsch et al., 2007), as the activity of ISCs, IHCs, and SGNs is highly correlated, and spontaneous burst firing in IHCs and SGNs is blocked by purinergic receptor antagonists. However, recent studies have reported that the effects of ATP are variable, inducing depolarization or hyperpolarization depending on the experimental conditions (Johnson et al., 2011), and that inhibition of purinergic receptors can lead to IHC excitation (Johnson et al., 2011).

Here we demonstrate that periodic excitation of IHCs is promoted by the buildup of K^+ around IHCs due to TMEM16A-mediated Cl^- efflux from nearby ISCs. This mechanism is consistent with many unusual aspects of spontaneous activity in the prehearing cochlea, including the slow kinetics of the responses, the appearance of depolarizing waves simultaneously in ISCs, IHCs, and SGN dendritic boutons, the enhancement of spontaneous and evoked release from cholinergic efferent terminals during ATP-induced events, the high correlation between ISC crenation and IHC/SGN activity, the spread of IHC activity beyond the region of activated ISCs, the sensitivity of these responses to antagonists of purinergic receptors and Cl^- channels, and the reduction in IHC activity when K^+ channels are inhibited. The developmental expression of TMEM16A follows the appearance of ISC crenation and IHC activity, and the expression of this channel is highly expressed by ISCs immediately adjacent to IHCs. The profound reduction in IHC activity in mice lacking TMEM16A, despite their homeostatic increase in excitability, indicates that ISCs play a crucial role in the generation of spontaneous burst firing before hearing onset. This identification of TMEM16A as a key molecular component of the pathway responsible for initiating synchronous activation of IHCs provides new opportunities to understand the functional roles of spontaneous activity in development of the auditory system.

EXPERIMENTAL PROCEDURES

Animals

All experiments were performed in accordance with protocols approved by the Animal Care and Use Committee at Johns Hopkins University. P5 to P10 Sprague Dawley rat pups (Charles River Laboratories) and mouse pups were used for experiments. The *Tecta-EGFP* mouse line was generated by modifying a BAC clone (RP23-217M9, BACPAC resource center, CHORI) using homologous recombination to insert a cDNA encoding EGFP followed by a rabbit β-globin poly A sequence at the start codon in exon 2 of α-tectorin gene. The linearized BAC preserved 62 kb upstream of the ATG and 66 kb downstream of the last coding exon. The BAC transgene was injected into pronuclei of one- or two-cell stage embryos of Friend virus B-type (FVB) mice and implanted into pseudo-pregnant female mice. Generic GFP primers were used for genotyping. *Pax2-Cre* mice (Ohyama and Groves, 2004), *Tmem16a:GFP* mice (Huang et al., 2012b), *Tmem16a* floxed mice (Schreiber et al., 2015), and *R26-lsl-GCaMP3* (Paukert et al., 2014) mice have been reported previously, and *Atoh1-Cre* transgenic mice (Matei et al., 2005) were obtained from Jackson Laboratory (011104). *Tmem16a* complete KO mice were generated by crossing *Tmem16a*$^{f/f}$ mice with *Sox2-Cre* transgenic mice (Jackson Laboratory: 004783) to obtain heterozygous-null mutant; these mice were subsequently interbred to obtain *Tmem16a* complete KO mice.

Data Analysis

Currents and potentials were recorded with pClamp9 software using a Multiclamp 700A amplifier (Molecular Devices), and data were analyzed offline using Clampfit 9 (Molecular Devices) and Origin 8 (OriginLab Co*rporation)* software. Data were presented as mean ± SEM. Statistical tests were performed using either paired two-tail student's t test or one-way ANOVA with Bonferroni's post hoc test, with significance determined by p value < 0.05. GCaMP3 fluorescence was imaged at 1 Hz for 10 min with a laser scanning confocal microscope (LSM 710; Zeiss) using a 20× water-immersion objective, 488 nm laser illumination, and 493–630 nm bandpass filter. The frequency and area of spontaneous Ca^{2+} transients were measured using ImageJ software (NIH).

For detailed information, please see Supplemental Experimental Procedures

SUPPLEMENTAL INFORMATION

Supplemental Information includes Supplemental Experimental Procedures, six figures, and three movies and can be found with this article online at http://dx.doi.org/10.1016/j.cell.2015.10.070.

AUTHOR CONTRIBUTIONS

H.C.W. and D.E.B. designed the experiments, H.C.W. performed the experiments, and H.C.W. and D.E.B. wrote the manuscript. C.-C.L. performed key preliminary studies, R.C. and Y.Z.-H. generated and characterized the *Tecta-EGFP* mice, and A.A. provided assistance with GCaMP3 imaging. G.E.-D. provided DMNPE-4/AM and J.R. provided both *Tmem16a:GFP* and *Tmem16a*$^{f/f}$ mouse lines.

ACKNOWLEDGMENTS

The authors thank Dr. Angelika Doetzlhofer for assistance with in situ hybridization and members of the Bergles laboratory for helpful discussions. Supported by grants from the NIH (NS050274, MH084020, DC008860 for D.E.B. and GM053395, NS06972 for G.E.-D.).

Received: May 26, 2015
Revised: September 10, 2015
Accepted: October 19, 2015
Published: November 25, 2015

REFERENCES

Blankenship, A.G., and Feller, M.B. (2010). Mechanisms underlying spontaneous patterned activity in developing neural circuits. Nat. Rev. Neurosci. *11*, 18–29.

Burnstock, G. (2007). Purine and pyrimidine receptors. Cell. Mol. Life Sci. *64*, 1471–1483.

Burnstock, G., and Williams, M. (2000). P2 purinergic receptors: modulation of cell function and therapeutic potential. J. Pharmacol. Exp. Ther. *295*, 862–869.

Clause, A., Kim, G., Sonntag, M., Weisz, C.J., Vetter, D.E., Rűbsamen, R., and Kandler, K. (2014). The precise temporal pattern of prehearing spontaneous activity is necessary for tonotopic map refinement. Neuron *82*, 822–835.

Eskandari, S., Zampighi, G.A., Leung, D.W., Wright, E.M., and Loo, D.D. (2002). Inhibition of gap junction hemichannels by chloride channel blockers. J. Membr. Biol. *185*, 93–102.

Freyer, L., Aggarwal, V., and Morrow, B.E. (2011). Dual embryonic origin of the mammalian otic vesicle forming the inner ear. Development *138*, 5403–5414.

Frizzell, R.A., and Hanrahan, J.W. (2012). Physiology of epithelial chloride and fluid secretion. Cold Spring Harb. Perspect. Med. *2*, a009563.

Glowatzki, E., and Fuchs, P.A. (2000). Cholinergic synaptic inhibition of inner hair cells in the neonatal mammalian cochlea. Science *288*, 2366–2368.

Glowatzki, E., and Fuchs, P.A. (2002). Transmitter release at the hair cell ribbon synapse. Nat. Neurosci. *5*, 147–154.

Glowatzki, E., Cheng, N., Hiel, H., Yi, E., Tanaka, K., Ellis-Davies, G.C., Rothstein, J.D., and Bergles, D.E. (2006). The glutamate-aspartate transporter GLAST mediates glutamate uptake at inner hair cell afferent synapses in the mammalian cochlea. J. Neurosci. *26*, 7659–7664.

Gordon, G.R., Choi, H.B., Rungta, R.L., Ellis-Davies, G.C., and MacVicar, B.A. (2008). Brain metabolism dictates the polarity of astrocyte control over arterioles. Nature *456*, 745–749.

Gulley, R.L., and Reese, T.S. (1976). Intercellular junctions in the reticular lamina of the organ of Corti. J. Neurocytol. *5*, 479–507.

Hoffmann, E.K., Lambert, I.H., and Pedersen, S.F. (2009). Physiology of cell volume regulation in vertebrates. Physiol. Rev. *89*, 193–277.

Housley, G.D., Bringmann, A., and Reichenbach, A. (2009). Purinergic signaling in special senses. Trends Neurosci. *32*, 128–141.

Huang, L.C., Thorne, P.R., Vlajkovic, S.M., and Housley, G.D. (2010). Differential expression of P2Y receptors in the rat cochlea during development. Purinergic Signal. *6*, 231–248.

Huang, F., Wong, X., and Jan, L.Y. (2012a). International Union of Basic and Clinical Pharmacology. LXXXV: calcium-activated chloride channels. Pharmacol. Rev. *64*, 1–15.

Huang, F., Zhang, H., Wu, M., Yang, H., Kudo, M., Peters, C.J., Woodruff, P.G., Solberg, O.D., Donne, M.L., Huang, X., et al. (2012b). Calcium-activated chloride channel TMEM16A modulates mucin secretion and airway smooth muscle contraction. Proc. Natl. Acad. Sci. USA *109*, 16354–16359.

Ito, K., and Dulon, D. (2010). Purinergic signaling in cochleovestibular hair cells and afferent neurons. Purinergic Signal. *6*, 201–209.

Jagger, D.J., and Forge, A. (2006). Compartmentalized and signal-selective gap junctional coupling in the hearing cochlea. J. Neurosci. *26*, 1260–1268.

Johnson, S.L., Eckrich, T., Kuhn, S., Zampini, V., Franz, C., Ranatunga, K.M., Roberts, T.P., Masetto, S., Knipper, M., Kros, C.J., and Marcotti, W. (2011). Position-dependent patterning of spontaneous action potentials in immature cochlear inner hair cells. Nat. Neurosci. *14*, 711–717.

Kelley, M.W. (2006). Regulation of cell fate in the sensory epithelia of the inner ear. Nat. Rev. Neurosci. *7*, 837–849.

Kirkby, L.A., Sack, G.S., Firl, A., and Feller, M.B. (2013). A role for correlated spontaneous activity in the assembly of neural circuits. Neuron *80*, 1129–1144.

Kofuji, P., and Newman, E.A. (2004). Potassium buffering in the central nervous system. Neuroscience *129*, 1045–1056.

Kros, C.J. (2007). How to build an inner hair cell: challenges for regeneration. Hear. Res. *227*, 3–10.

Kros, C.J., Ruppersberg, J.P., and Rüsch, A. (1998). Expression of a potassium current in inner hair cells during development of hearing in mice. Nature *394*, 281–284.

Lippe, W.R. (1994). Rhythmic spontaneous activity in the developing avian auditory system. J. Neurosci. *14*, 1486–1495.

Matei, V., Pauley, S., Kaing, S., Rowitch, D., Beisel, K.W., Morris, K., Feng, F., Jones, K., Lee, J., and Fritzsch, B. (2005). Smaller inner ear sensory epithelia in Neurog 1 null mice are related to earlier hair cell cycle exit. Dev. Dyn. *234*, 633–650.

Moody, W.J., and Bosma, M.M. (2005). Ion channel development, spontaneous activity, and activity-dependent development in nerve and muscle cells. Physiol. Rev. *85*, 883–941.

Novak, I. (2011). Purinergic signalling in epithelial ion transport: regulation of secretion and absorption. Acta Physiol. (Oxf.) *202*, 501–522.

Ohyama, T., and Groves, A.K. (2004). Generation of Pax2-Cre mice by modification of a Pax2 bacterial artificial chromosome. Genesis *38*, 195–199.

Paukert, M., Agarwal, A., Cha, J., Doze, V.A., Kang, J.U., and Bergles, D.E. (2014). Norepinephrine controls astroglial responsiveness to local circuit activity. Neuron *82*, 1263–1270.

Rau, A., Legan, P.K., and Richardson, G.P. (1999). Tectorin mRNA expression is spatially and temporally restricted during mouse inner ear development. J. Comp. Neurol. *405*, 271–280.

Rock, J.R., Futtner, C.R., and Harfe, B.D. (2008). The transmembrane protein TMEM16A is required for normal development of the murine trachea. Dev. Biol. *321*, 141–149.

Scheffer, D.I., Shen, J., Corey, D.P., and Chen, Z.-Y. (2015). Gene Expression by Mouse Inner Ear Hair Cells during Development. J. Neurosci. *35*, 6366–6380.

Schreiber, R., Faria, D., Skryabin, B.V., Wanitchakool, P., Rock, J.R., and Kunzelmann, K. (2015). Anoctamins support calcium-dependent chloride secretion by facilitating calcium signaling in adult mouse intestine. Pflugers Arch. *467*, 1203–1213.

Sendin, G., Bourien, J., Rassendren, F., Puel, J.L., and Nouvian, R. (2014). Spatiotemporal pattern of action potential firing in developing inner hair cells of the mouse cochlea. Proc. Natl. Acad. Sci. USA *111*, 1999–2004.

Sobkowicz, H.M., Rose, J.E., Scott, G.E., and Slapnick, S.M. (1982). Ribbon synapses in the developing intact and cultured organ of Corti in the mouse. J. Neurosci. *2*, 942–957.

Sugasawa, M., Erostegui, C., Blanchet, C., and Dulon, D. (1996). ATP activates a cation conductance and $Ca^{(2+)}$-dependent Cl^- conductance in Hensen cells of guinea pig cochlea. Am. J. Physiol. *271*, C1817–C1827.

Tritsch, N.X., and Bergles, D.E. (2010). Developmental regulation of spontaneous activity in the Mammalian cochlea. J. Neurosci. *30*, 1539–1550.

Tritsch, N.X., Yi, E., Gale, J.E., Glowatzki, E., and Bergles, D.E. (2007). The origin of spontaneous activity in the developing auditory system. Nature *450*, 50–55.

Tritsch, N.X., Rodríguez-Contreras, A., Crins, T.T., Wang, H.C., Borst, J.G., and Bergles, D.E. (2010a). Calcium action potentials in hair cells pattern auditory neuron activity before hearing onset. Nat. Neurosci. *13*, 1050–1052.

Tritsch, N.X., Zhang, Y.X., Ellis-Davies, G., and Bergles, D.E. (2010b). ATP-induced morphological changes in supporting cells of the developing cochlea. Purinergic Signal. *6*, 155–166.

Wang, H.C., and Bergles, D.E. (2015). Spontaneous activity in the developing auditory system. Cell Tissue Res. *361*, 65–75.

Yi, E., Lee, J., and Lee, C.J. (2013). Developmental Role of Anoctamin-1/TMEM16A in $Ca^{(2+)}$-Dependent Volume Change in Supporting Cells of the Mouse Cochlea. Exp. Neurobiol. *22*, 322–329.